Article

Interplay between Size and Electronic Effects in Determining the Homogeneity Range of the AZnPn and ACdPn Phases (0 ≤ *x* ≤ 0.5), A = Ca, Sr, Yb, Eu; Pn = Sb, Bi

Sheng-qing Xia, and Svilen Bobev

J. Am. Chem. Soc., **2007**, 129 (32), 10011-10018• DOI: 10.1021/ja0728425 • Publication Date (Web): 21 July 2007

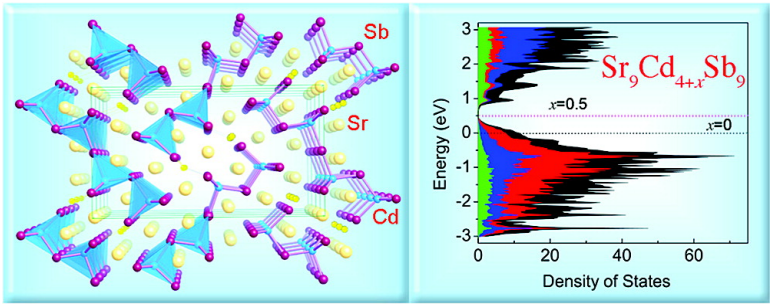

More About This Article

Additional resources and features associated with this article are available within the HTML version:

- Supporting Information
- Links to the 5 articles that cite this article, as of the time of this article download
- Access to high resolution figures
- Links to articles and content related to this article
- Copyright permission to reproduce figures and/or text from this article

View the Full Text HTML

J|A|C|S
ARTICLES
Published on Web 07/21/2007

Interplay between Size and Electronic Effects in Determining the Homogeneity Range of the $A_9Zn_{4+x}Pn_9$ and $A_9Cd_{4+x}Pn_9$ Phases ($0 \leq x \leq 0.5$), A = Ca, Sr, Yb, Eu; Pn = Sb, Bi

Sheng-qing Xia and Svilen Bobev*

Contribution from the Department of Chemistry and Biochemistry, University of Delaware, Newark, Delaware 19716

Received April 23, 2007; E-mail: bobev@udel.edu

Abstract: Seven cadmium- and zinc-containing Zintl phases, $A_9Zn_{4+x}Pn_9$ and $A_9Cd_{4+x}Pn_9$ ($0 \leq x \leq 0.5$), A = Ca, Sr, Yb, Eu; Pn = Sb, Bi, have been synthesized, and their structures have been determined by single-crystal X-ray diffraction. All compounds are isostructural and crystallize in the centrosymmetric orthorhombic space group *Pbam* (no. 55, $Z = 2$), and their structures feature tetrahedra of the pnicogens, centered by the transition metal. The tetrahedra are not isolated but are connected through corner sharing to form ribbons, which are separated by the divalent cations. The occurrence of a small phase width and its variation across this family of compounds has been systematically studied by variable temperature crystallography, resistivity, and magnetic susceptibility measurements, and these results have been reconciled with electronic structure calculations performed using the tight-binding linear muffin-tin orbital (TB−LMTO−ASA) method. These analyses of the crystal and electronic structure indicate that the polyanionic subnetwork requires 19 additional electrons, whereas only 18 electrons are provided by the cations. Such apparent "electron deficiency" necessitates the presence of an interstitial atom in order for an optimal bonding to be achieved; however, an interplay between the sizes of the cations and anions and the total valence electron concentration (governed by the stoichiometry breadth) is suggested as a possible mechanism for achieving structure stability. The structural relationship between these and some known structures with two-dimensional layers are discussed as well.

Introduction

The crystal chemistry of the intermetallic compounds containing metals with very different electronegativities presents a combination of diverse and complicated bonding patterns and unique metal−metal interactions that are not characteristic of the typical covalent or ionic solids.[1] As a result, such compounds exhibit a variety of unprecedented physical properties, which have captured the attention of many researchers around the globe.[1−8] The rich phenomenology of these systems spans the full breadth of solid-state research from chemistry to physics to materials science;[1−8] however, despite the tremendous information gathered to date, their complicated crystal and electronic structures continue to pose serious difficulties in rationalizing the structure−property relationships.

In most simplified terms, the main factors that govern the formation, stability, and properties of the intermetallic phases are (i) the relative sizes (a.k.a. size effects) and (ii) an interplay of the relative electronegativities and number of valence electrons of the constituent atoms (a.k.a. electronic effects). Several classic concepts use these as underlying principles, such as the ideas of Zintl, Laves, Hume-Rothery, and Pearson, among others, which prove very effective in rationalizing the structures of specific classes of compounds.[9] In many cases, however, the bonding interactions are intermediate between the localized two-center−two-electron and the delocalized multicenter bonding,

(1) (a) Corbett, J. D. *Angew. Chem., Int. Ed.* **2000**, *39*, 670−690. (b) Kauzlarich, S. M., Ed. *Chemistry, Structure and Bonding in Zintl Phases and Ions*; VCH: New York, 1996 and the references therein.
(2) (a) Lee, C. S.; Miller, G. J. *J. Am. Chem. Soc.* **2000**, *122*, 4937−4947. (b) Haussermann, U.; Amerioun, S.; Eriksson, L.; Lee, C. S.; Miller, G. J. *J. Am. Chem. Soc.* **2002**, *124*, 4371−4383. (c) Mozharivskyj, Y.; Choe, W.; Pecharsky, A. O.; Miller, G. J. *J. Am. Chem. Soc.* **2003**, *125*, 15183−15190.
(3) (a) Goodey, J.; Mao, J.-G.; Guloy, A. M. *J. Am. Chem. Soc.* **2000**, *122*, 10478−10479. (b) Lupu, C.; Downie, C.; Guloy, A. M.; Albright, T. A.; Mao, J.-G. *J. Am. Chem. Soc.* **2004**, *126*, 4386−4397.
(4) (a) Chen, L.; Corbett, J. D. *J. Am. Chem. Soc.* **2003**, *125*, 1170−1171. (b) Li, B.; Corbett, J. D. *J. Am. Chem. Soc.* **2005**, *127*, 926−932. (c) Chen, L.; Corbett, J. D. *J. Am. Chem. Soc.* **2003**, *125*, 7794−7795. (d) Li, B.; Corbett, J. D. *J. Am. Chem. Soc.* **2006**, *128*, 12392−12393.
(5) (a) Houben, A.; Müller, P.; von Appen, J.; Lueken, H.; Niewa, R.; Dronskowski, R. *Angew. Chem., Int. Ed.* **2005**, *44*, 7212−7215. (b) von Appen, J.; Dronskowski, R. *Angew. Chem., Int. Ed.* **2005**, *44*, 1205−1210.
(6) (a) Poudeu, P. F. P.; D'Angelo, J.; Kong, H. J.; Downey, A.; Short, J. L.; Pcionek, R.; Hogan, T. P.; Uher, C.; Kanatzidis, M. G. *J. Am. Chem. Soc.* **2006**, *128*, 14347−14355. (b) Park, S. M.; Kim, S. J.; Kanatzidis, M. G. *Inorg. Chem.* **2005**, *44*, 4979−4982. (c) Kim, S. J.; Salvador, J.; Bilc, D.; Mahanti, S. D.; Kanatzidis, M. G. *J. Am. Chem. Soc.* **2001**, *123*, 12704−12705. (d) Chung, D.-Y.; Hogan, T.; Brazis, P.; Rocci-Lane, M.; Kannewurf, C.; Bastea, M.; Uher, C.; Kanatzidis, M. G. *Science* **2000**, *287*, 1024−1027.
(7) (a) Kuromoto, T. Y.; Kauzlarich, S. M.; Webb, D. J. *Chem. Mater.* **1992**, *4*, 435−440. (b) Young, D. M.; Torardi, C. C.; Olmstead, M. M.; Kauzlarich, S. M. *Chem. Mater.* **1995**, *7*, 93−101. (c) Jiang, J.; Payne, A. C.; Olmstead, M. M.; Lee, H. O.; Klavins, P.; Fisk, Z.; Kauzlarich, S. M.; Hermann, R. P.; Grandjean, F.; Long, G. J. *Inorg. Chem.* **2005**, *44*, 2189−2197. (d) Brown, S. R.; Kauzlarich, S. M.; Gascoin, F.; Snyder, G. J. *Chem. Mater.* **2006**, *18*, 1873−1877.
(8) (a) Bobev, S.; Merz, J.; Lima, A.; Fritsch, V.; Thompson, J. D.; Sarrao, J. L.; Gillessen, M.; Dronskowski, R. *Inorg. Chem.* **2006**, *45*, 4047−4054. (b) Xia, S.-Q.; Bobev, S. *J. Solid State Chem.* **2006**, *179*, 3371−3377. (c) Xia, S.-Q.; Bobev, S. *Inorg. Chem.* **2006**, *45*, 7126−7132. (d) Xia, S.-Q.; Bobev, S. *Inorg. Chem.* **2007**, *46*, 874−883.

rendering these rules inadequate. Examples abound where deviations from the optimal electron count are compensated by an interplay of the Madelung (lattice) energy and the size effects.[10]

As part of a broad effort to better understand the structure−property relationships in intermetallics containing d-block and/or f-block elements, we focused our attention on systems with one- or two-dimensional networks.[8,11] Recently, we reported two new Zintl compounds, Yb_2CdSb_2 and Ca_2CdSb_2, whose formation seems to be governed by factors that are different than the above-described ones.[12] These structures are both based on corner-shared $CdSb_4$ tetrahedra forming layers with the same connectivity; however, regardless of the identical electronic requirements and sizes of the cations, their packing is different. This rather surprising finding is supported by electronic structure calculations, which also indicate strong cation preference for each arrangement.

In an attempt to extend these studies toward Sr_2CdSb_2 and various other Bi analogs, we discovered several new compounds, $Sr_9Cd_{4+x}Sb_9$, $A_9Zn_{4+x}Bi_9$, and $A_9Cd_{4+x}Bi_9$ ($0 < x < 0.5$; A = Ca, Sr, Eu, Yb), the structures and compositions of which resemble closely those of Yb_2CdSb_2 and Ca_2CdSb_2. Herein, we report the synthesis, structural characterization, and properties of this series of compounds. The discussed analyses of the crystal structure, alongside the band structure calculated using the linear muffin-tin orbital method (LMTO), provide an example of a delicate balance between the size and the electronic effects (above). Such an interplay not only impacts the phase stability but also helps rationalize the existence of homogeneity range in these phases. In the last section of the article, these results are discussed in a broader prospective and put into the context of cation−anion interactions as important structure- and property-determining factors in such systems.[13] The present study also compliments the results from our previous work on $Yb_9Zn_{4+x}Sb_9$ and $Ca_9Zn_{4+x}Sb_9$[11] and confirms that the entire family of phases that are closely related to $Ca_9Mn_4Bi_9$ (Pearson's symbol *oP*44),[14] are *not* fully stoichiometric compounds.

Experimental Section

Synthesis. Handling of all materials was carried out inside an argon-filled glovebox or under vacuum. All elements for the syntheses were with purity greater than 99.9% (metal basis) and were used as received. Two different synthetic routes were explored—on-stoichiometry reactions in welded Nb tubes and flux reactions in alumina crucibles. Since the following discussions on the structure and the bonding are based on one representative only, $Sr_9Cd_{4.49(1)}Sb_9$, a brief summary of the synthesis of this compound is given below. The general experimental procedures and temperature profiles for the remaining isostructural compounds, along with specific details on the techniques, are described as Supporting Information.

$Sr_9Cd_{4.49(1)}Sb_9$ was initially synthesized from a reaction intended to produce Sr_2CdSb_2, isostructural with the recently reported Ca_2CdSb_2.[12] For this purpose, the lead flux method was employed.[15] The optimized reaction conditions were as follows: Sr, Cd, Sb, and Pb in a ratio 2:1:2:10 were loaded in alumina crucibles, which were in turn enclosed in evacuated fused-silica ampoules. The reaction mixture was heated from room temperature to 960 °C at a rate of 200 °C/h, allowed to dwell at this temperature for 20 h, and then slowly cooled to 500 °C at a rate of 5 °C/h. At this temperature the molten Pb was removed, and the needle-like crystals were isolated. They appeared dark and very brittle and quickly lost their metallic luster upon exposure to air.

In an attempt to probe the possible phase width in this system, a different reaction methodology was utilized. It included weighing the elements in the ratio of Sr:Cd:Sb = 9:4:9 and loading the mixture in a Nb tube, which was subsequently arc-welded at both ends under argon atmosphere. Next, the welded niobium container was enclosed in a fused-silica tube, which was evacuated to 10^{-5} torr (below discharge) and flame-sealed. The reaction mixture was heated from room temperature to 1000 °C at a rate of 200 °C/h, allowed to dwell at this temperature for 24 h, then slowly cooled down to 800 °C at a rate of 3 °C/h. At this temperature, there was a second dwell step for 72 h, followed by a cooling step to room temperature at a rate of 3 °C/h. The single crystals obtained by this reaction were small and irregularly shaped but were of excellent crystallographic quality. According to the X-ray powder pattern, $Sr_9Cd_{4.49(1)}Sb_9$ was the major product of this reaction.

The crystallographic data discussed herein are based on the "on-stoichiometry" synthesized sample of $Sr_9Cd_{4.49(1)}Sb_9$. The data obtained from crystals grown in Pb flux are in excellent agreement with the latter and are provided in the Supporting Information.

Powder X-ray Diffraction. X-ray powder diffraction patterns were taken at room temperature on a Rigaku MiniFlex powder diffractometer, operated at 0.45 kW and using Ni-filtered Cu Kα radiation. The diffractometer was enclosed in a glovebox in order to allow for the identification of air- or moisture-sensitive materials. Data were collected in a $\theta-\theta$ mode ($2\theta_{max} = 80°$) with a step size of 0.02° and 10 s/step counting time. The data analysis was carried out using the JADE 6.5 software package. The position and the intensity of the peaks matched fairly well with those calculated from the refined structures. The limited instrument resolution and the fairly large unit cell parameters for the title compounds resulted in powder patterns with many peaks, some of which overlapped. This complicated the analyses of the phase purity and precluded the straightforward determination of the unit cell constants from powder diffraction data. Therefore, all cell parameters reported herein (see also the Supporting Information) were determined and refined from single-crystal X-ray diffraction data.

Single-Crystal X-ray Diffraction. All intensity data collections were handled routinely. Provided herein are relevant details for $Sr_9Cd_{4.49(1)}Sb_9$ only, the structure of which is discussed at length in the next section. Detailed information for all other crystal structures is given as Supporting Information.

Because of the sensitivity to air of the $Sr_9Cd_{4.49(1)}Sb_9$ compound, a suitable single crystal was selected in the glovebox and cut to $0.06 \times 0.05 \times 0.04$ mm^3 dimensions. The crystal was removed from the glovebox and quickly mounted on a glass fiber using Paratone N oil and placed under the cold nitrogen stream (ca. −153 °C) of the goniometer of a Bruker SMART CCD-based diffractometer. Intensity data covering a full sphere of the reciprocal space were collected in four batch runs at different ω and ϕ angles. Frame width was 0.4° in ω and θ and the acquisition rate was 15 s/frame. The data collection, data integration, and cell refinement were done using the SMART and SAINT programs,[16] respectively. Semiempirical absorption correction

(9) (a) Zintl, E. *Angew. Chem.* **1939**, *52*, 1−6. (b) Nesper, R. *Prog. Solid State Chem.* **1990**, *20*, 1−45. (c) Nesper, R. *Angew. Chem., Int. Ed. Engl.* **1991**, *30*, 789−817.
(10) (a) Seo, D.-K.; Corbett, J. D. *J. Am. Chem. Soc.* **2000**, *122*, 9621−9627. (b) Seo, D.-K.; Corbett, J. D. *J. Am. Chem. Soc.* **2001**, *123*, 4512−4518. (c) Seo, D.-K.; Corbett, J. D. *J. Am. Chem. Soc.* **2002**, *124*, 415−420.
(11) Bobev, S.; Thompson, J. D.; Sarrao, J. L.; Olmstead, M. M.; Hope, H.; Kauzlarich, S. M. *Inorg. Chem.* **2004**, *43*, 5044−5052.
(12) Xia, S.-Q.; Bobev, S. *J. Am. Chem. Soc.* **2007**, *129*, 4049−4057.
(13) (a) Liu, S.-F.; Corbett, J. D. *Inorg. Chem.* **2004**, *43*, 4988−4993. (b) Li, B.; Corbett, J. D. *Inorg. Chem.* **2006**, *45*, 8958−8964. (c) Li, B.; Corbett, J. D. *Inorg. Chem.* **2007**, *46*, 2237−2242.
(14) (a) Brechtel, E.; Cordier, G.; Schäfer, H. *Z. Naturforsch.* **1979**, *34B*, 1229−1233. (b) Brechtel, E.; Cordier, G.; Schäfer, H. *Z. Naturforsch.* **1981**, *36B*, 1099−1104.
(15) Kanatzidis, M. G.; Pöttgen, R.; Jeitschko, W. *Angew. Chem., Int. Ed.* **2005**, *44*, 6996−7023.
(16) *SMART* and *SAINT*; Bruker AXS Inc.: Madison, WI, 2002.

Table 1. Selected Crystal Data and Structure Refinement Parameters for $Sr_9Cd_{4.49(1)}Sb_9$

empirical formula	$Sr_9Cd_{4.49(1)}Sb_9$
formula weight	2389.57 g/mol
data collection temperature	−153(2) °C
radiation, wavelength	Mo Kα, $\lambda = 0.71073$ Å
crystal system	orthorhombic
space group	*Pbam* (no. 55)
unit cell dimensions	$a = 23.181(2)$ Å
	$b = 13.0498(13)$ Å
	$c = 4.7950(5)$ Å
unit cell volume, Z	1450.5(3) Å^3, 2
density (ρ_{calc})	5.471 g/cm^3
absorption coefficient (μ)	27.805 mm^{-1}
goodness-of-fit	1.148
final R indices [$I > 2\sigma_{(I)}$][a]	$R_1 = 0.0263$
	$wR_2 = 0.0516$
final R indices [all data][a]	$R_1 = 0.0299$
	wR2 = 0.0526

[a] $R_1 = \sum||F_o| - |F_c||/\sum|F_o|$; $wR_2 = [\sum[w(F_o^2 - F_c^2)^2]/\sum[w(F_o^2)^2]]^{1/2}$, where $w = 1/[\sigma^2F_o^2 + (0.018P)^2 + 7.525P]$, $P = (F_o^2 + 2F_c^2)/3$.

based on equivalents ($T_{min}/T_{max} = 0.672$) was applied with the aid of SADABS.[17]

Analysis of the reflection conditions suggested the centrosymmetric space group *Pbam* (no. 55), and the structure was readily solved by direct methods. All sites in the asymmetric unit, excluding one of the cadmiums, were located from the solution. Subsequent refinement by the full matrix least-squares on F^2 method (using SHELXL[18]) indicated a residual peak of ca. 30 e$^-$/Å^3, located approximately 2.7 Å away from Sb2 and Sb4. In analogy with the structures of $Yb_9Zn_{4+x}Sb_9$ and $Ca_9Zn_{4+x}Sb_9$ ($x \approx 0.5$),[11] this site was assigned as partially occupied Cd (Cd3, refined occupancy of 24.6(3)%).[19] Following structure refinements, where all atoms including the partially occupied Cd3 were refined with anisotropic displacement parameters, converged at low conventional R values and featureless final difference Fourier map (see the Supporting Information for a representative plot with thermal ellipsoids). Additional details on the data collection and structure refinement parameters are given in Table 1.

In the last refinement cycles, the atomic positions and labels were unified with those from the previously reported structures.[11] Final positional and equivalent isotropic displacement parameters and important bond distances and angles are listed in Tables 2 and 3, respectively. Further information in the form of CIF has been deposited with FIZ Karlsruhe, 76344 Eggenstein-Leopoldshafen, Germany, (e-mail: crysdata@fiz. karlsruhe.de)—depository number CSD 417974 ($Sr_9Cd_{4.49(1)}Sb_9$).[20]

Property Measurements. Field-cooling dc magnetization measurements were performed in a Quantum Design MPMS SQUID magnetometer in an applied magnetic field of 500 Oe. Only the europium- and the ytterbium-containing compounds were measured. Due to their sensitivity to air, polycrystalline samples were prepared and weighed in the glovebox and enclosed in custom-designed holders made of fused-silica tubes (details on the design can be found elsewhere[8d]). The raw data were corrected for the holder's contribution and converted to molar susceptibility.

A large, needle-shaped single crystal of $Eu_9Cd_{4.21(1)}Bi_9$ was obtained from a flux reaction (above). It was used for a four-probe electrical resistivity measurement that was carried out along the needle direction (presumed to be the direction of the shortest crystallographic axis). This was the only compound for which reproducible data were obtained. Resistivity measurements for the remaining compounds proved unreliable—either because of lack of suitable single crystals or because of their much quicker decomposition upon exposure to air. A representative plot of the temperature dependence of the resistivity of $Eu_9Cd_{4.21(1)}Bi_9$ is provided as Supporting Information.

Table 2. Atomic Coordinates and Equivalent Isotropic Displacement Parameters (U_{eq}) for $Sr_9Cd_{4.49(1)}Sb_9$

atom	Wyckoff position	x	y	z	U_{eq}[a] [Å^2]
Sb1	2*d*	0	1/2	1/2	0.0099(2)
Sb2	4*g*	0.49548(3)	0.30832(5)	0	0.0119(1)
Sb3	4*g*	0.30623(3)	0.12885(5)	0	0.0140(2)
Sb4	4*h*	0.35101(3)	0.46320(4)	1/2	0.0096(1)
Sb5	4*h*	0.16536(3)	0.31295(4)	1/2	0.0084(1)
Cd1	4*h*	0.04406(3)	0.27985(5)	1/2	0.0119(2)
Cd2	4*h*	0.24000(3)	0.12386(5)	1/2	0.0120(2)
Cd3[b]	4*g*	0.3924(1)	0.3853(3)	0	0.024(1)
Sr1	2*b*	0	0	1/2	0.0127(3)
Sr2	4*g*	0.13570(4)	0.13865(6)	0	0.0107(2)
Sr3	4*g*	0.09120(4)	0.44633(7)	0	0.0102(2)
Sr4	4*g*	0.25929(4)	0.38116(7)	0	0.0140(2)
Sr5	4*h*	0.39599(4)	0.21608(7)	1/2	0.0192(2)

[a] U_{eq} is defined as one-third of the trace of the orthogonalized U_{ij} tensor. [b] Refined occupancy is 0.246(3).

Table 3. Side-by-Side Comparison of Some Relevant Bond Distances (angstroms) and Bond Angles (deg) in $Sr_9Cd_{4.49(1)}Sb_9$ and Ca_2CdSb_2

$Sr_9Cd_{4.49(1)}Sb_9$		Ca_2CdSb_2	
Sb2−Cd1 × 2	2.8878(6)	Sb2−Cd × 2	2.8226(5)
Sb3−Cd2 × 2	2.8477(5)	Sb2−Cd × 2	2.8226(5)
Sb4−Cd2	2.9744(9)	Sb1−Cd	3.0054(8)
Sb5−Cd1	2.8447(9)	Sb1−Cd	3.0054(8)
Sb5−Cd2	3.0137(9)	Sb1−Cd	2.8981(8)
Sb2−Cd1 × 2	2.8878(6)	Sb2−Cd × 2	2.8226(5)
Sr2−Sb2	3.3232(11)	Ca2−Sb2	3.1323(14)
Sb3	3.9551(11)	Sb2	4.102(2)
Sb4 × 2	3.3294(8)	Sb1 × 2	3.1682(10)
Cd1−Sb2−Cd1	112.24(3)	Cd−Sb2−Cd	109.25(2)
Cd2−Sb3−Cd2	114.68(3)	Cd−Sb2−Cd	109.25(2)
Cd1−Sb5−Cd2	116.31(3)	Cd−Sb1−Cd	116.652(19)
Sb2−Cd1−Sb5	116.48(2)	Sb1−Cd−Sb2	113.331(14)
Sb4−Cd2−Sb5	99.78(3)	Sb1−Cd−Sb1	93.695(17)

Electronic Structure Calculations. Electronic structure calculations were performed using the TB−LMTO program.[21] Exchange and correlation were treated in the local density approximation (LDA).[22] All relativistic effects except for spin−orbit coupling were taken into account by the scalar relativistic approximation.[23] The basis set included the 4d, 5s, and 5p orbitals for Sr, 4d, 5s, and 5p orbitals for Cd, and 5s, 5p, and 5d orbitals for Sb. The Sr's 5p and the Sb's 5d orbitals were downfolded.[24] The k-space integrations were performed by the tetrahedron method[25] using 360 k-points in the Brillouin zone. The Fermi level was selected as the energy reference ($\epsilon_F = 0$ eV).

(17) Sheldrick, G. M. SADABS. University of Göttingen, Germany, 2003.
(18) Sheldrick, G. M. SHELXTL. University of Göttingen, Germany, 2001.
(19) In previous studies (ref 11), the residual density was assigned as Zn, but light impurity atoms were never completely ruled out. In the present case, the fairly large occupancy of the interstitial site and the high scattering factor of Cd makes the distinction very clear. The results are reproducible not only for crystals synthesized from on-stoichiometry reactions, for example, the refined occupancy for a crystal grown from Pb flux is nearly identical—see the Supporting Information.
(20) Depository numbers for the remaining compounds: CSD 417973 ($Ca_9Cd_{4.06(1)}Bi_9$); CSD 417975 ($Eu_9Cd_{4.21(1)}Bi_9$); CSD 417976 ($Sr_9Cd_{4.26(2)}Bi_9$); CSD 417979 ($Yb_9Cd_{4.01(1)}Bi_9$); CSD 417978 ($Ca_9Zn_{4.10(1)}Bi_9$); CSD 417977 ($Yb_9Zn_{4.03(2)}Bi_9$).
(21) Jepsen, O.; Andersen, O. K. *The Stuttgart TB−LMTO Program*, version 4.7.
(22) Von Barth, U.; Hedin, L. *J. Phys. C: Solid State Phys.* **1972**, *5*, 1629−1642.
(23) Koelling, D. D.; Harmon, B. N. *J. Phys. C: Solid State Phys.* **1977**, *10*, 3107−3114.
(24) Lambrecht, W. R. L.; Andersen, O. K. *Phys. Rev. B* **1986**, *34*, 2439−2449.
(25) Blöchl, P. E.; Jepsen, O.; Andersen, O. K. *Phys. Rev. B.* **1994**, *49*, 16223−16233.

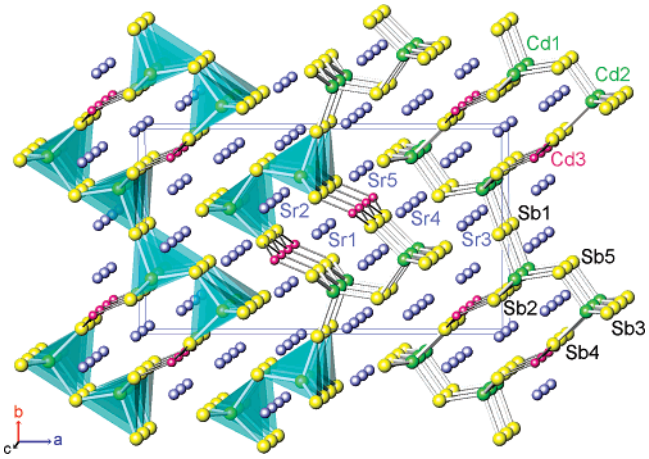

Figure 1. Polyhedral and ball-and-stick representation of the structure of $Sr_9Cd_{4.49(1)}Sb_9$ (*Pbam*), viewed approximately down the *c*-axis. The Sb atoms are drawn as yellow spheres, and the Cd atoms are shown as light-green spheres, which center the translucent tetrahedra, respectively. The Sr atoms are drawn as blue spheres, and the unit cell is outlined. The partially occupied cadmiums, Cd3, are shown as small red spheres.

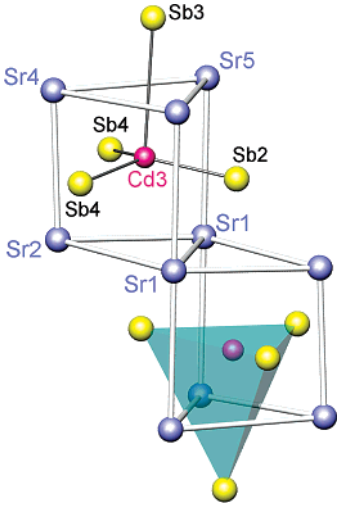

Figure 2. Close-up view of a coordination environment of Cd3.

Results and Discussion

Structure Description. The seven title compounds, $Sr_9Cd_{4+x}Sb_9$, $A_9Zn_{4+x}Bi_9$, and $A_9Cd_{4+x}Bi_9$ ($0 < x < 0.5$; A = Ca, Sr, Eu, Yb) crystallize with the orthorhombic space group *Pbam*, and their structures contain 13 crystallographically unique atoms in the asymmetric unit (5 pnicogen, 3 transition metal, and 5 alkaline- or rare-earth atoms), all of which are in special positions with $z = 0$ or $z = 1/2$ (Table 2). Formally, this atomic arrangement belongs to the $Ca_9Mn_4Bi_9$ type (Pearson's symbol *oP*44)[14] with an additional partially occupied site to explain the narrow homogeneity range. The recent report on the related $Ca_9Zn_{4+x}Sb_9$ and $Yb_9Zn_{4+x}Sb_9$ ($0 < x < 0.5$) compounds[11] has raised the issue whether or not a phase width exists for all members of this family; herein we provide additional evidence that resolves this unsettled ambiguity. These considerations are discussed in detail in the next paragraphs on the example of $Sr_9Cd_{4.49(1)}Sb_9$, for which this effect is most noticeable. The remaining six bismuthides follow the same trends, and specific points about them are addressed in the Supporting Information. Another reason for the choice of $Sr_9Cd_{4.49(1)}Sb_9$ as the focus of our attention here is its close structural relationship to the recently reported compound, Ca_2CdSb_2.[12] Since both compounds have Cd−Sb sublattices, the structures and the bonding in $Sr_9Cd_{4.49(1)}Sb_9$ and Ca_2CdSb_2 (note how close their compositions are) are considered side-by-side.

The polyanionic subnetwork in $Sr_9Cd_{4.49(1)}Sb_9$ is best described in terms of Cd-centered tetrahedra of Sb, which are joined together through common corners in two perpendicular directions: four such $CdSb_4$ tetrahedra are "connected" by glide symmetry in the *ab*-plane (Figure 1); the mirror symmetry along the *c*-axis "joins" these fragments into one-dimensional [Cd_4Sb_9] ribbons that run parallel to this direction as shown in Figure 1. Each of the ribbons is centered at one of the five Sb sites, Sb1 (Wyckoff letter 2*d*, point symmetry 2/*m*), which results in its rather unusual coordination—linear. This may account for the significant elongation of the Cd1−Sb1 bonds and the accompanying distortion of the neighboring bond angles (Table 3). The peculiarity of this crystallographic arrangement and its implication on the rationalization of the structure and the electron count has already been given a full consideration elsewhere;[11,14] we will refer again to these "nonclassical" interactions when discussing the electronic structure in the next section.

Another line of reasoning that deserves a special mention here is the interstitial cadmium site, Cd3 in the current notation (Table 2), and its coordination. It has a well-defined coordination sphere, and it centers a distorted trigonal prism formed by six strontium cations (Figure 2). The corresponding Cd−Sr distances range from 3.085(3) to 3.770(3) Å and fall within the expected range.[13,26] The faces of the prism are capped by antimony atoms, four of which form an irregular tetrahedron around the interstitial cadmium (Figure 2); another Sb atom is farther away ($d_{Cd-Sb} > 4.7$ Å). Three of the Cd−Sb distances within this tetrahedron are too short for normal Cd−Sb bonds ($d_{Cd3-Sb2}$ and $d_{Cd3-Sb4}$ are smaller than 2.78 Å), apparently an artifact of the one-quarter occupancy (or less) of the cadmium. These "unreal" distances can be interpreted if one recognizes that the majority (>75%) of the Sb2 atoms are actually *not* bonded to Cd3, the minority case when Cd3 and Sb2 form a bond is a perturbation and could be modeled with a small positional disorder. Analyses of the difference Fourier maps, calculated from low-temperature single-crystal X-ray diffraction data for the series $Yb_9Cd_{4.01(1)}Bi_9$, $Ca_9Cd_{4.06(1)}Bi_9$, $Eu_9Cd_{4.21(1)}Bi_9$, and $Sr_9Cd_{4.26(2)}Bi_9$, clearly show signs of disorder. Importantly, the displacement of the Bi2 from its ideal position correlates well with the increased Cd3 occupancy in the presented order (see the Supporting Information). Refining the Cd3−Bi2 pair with the disordered model yields even lower conventional *R* values and reasonable transition metal−pnicogen distances.

As already noted, the underoccupancy of the Cd3 site accounts for the "off-stoichiometry" in this family of compounds. We also emphasize that the homogeneity range is different for the different members (Tables 1 and S1); however the phase width in each case appears to be rather narrow—attempts to synthesize $Sr_9Cd_{4+x}Sb_9$, $A_9Zn_{4+x}Bi_9$, and $A_9Cd_{4+x}Bi_9$ where "*x*" varies significantly from the values reported herein were unsuccessful. These experimental facts combined

(26) Park, S.-M.; Kim, S.-J. *J. Solid State Chem.* **2004**, *177*, 3418−3422.

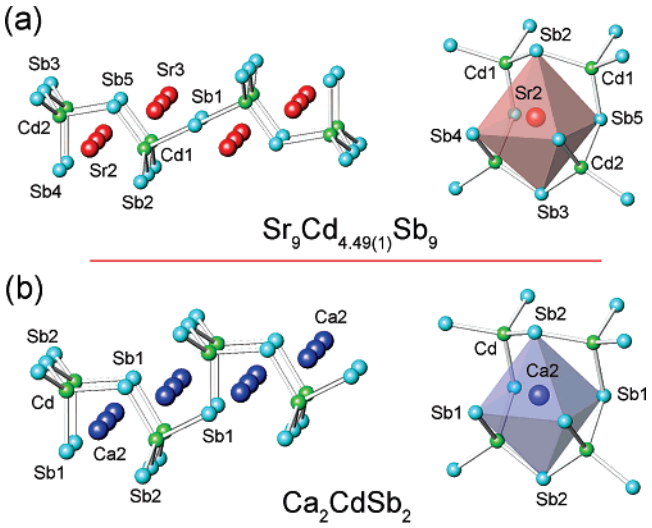

Figure 3. Side-by-side comparison of fragments of the $Sr_9Cd_{4.49(1)}Sb_9$ (a) and Ca_2CdSb_2 (b) structures. A formal removal of the center of symmetry and bending of the central Cd1−Sb1−Cd1 bond in (a) result in the same topology as in (b). See text for details.

with the analyses of the electronic structure and some geometric considerations corroborate the hypothesis that a small, but not negligible, homogeneity range exists, as suggested in the earlier study of $Yb_9Zn_{4+x}Sb_9$.[11] In the case of $Sr_9Cd_{4+x}Sb_9$, for example, invariably of the reaction conditions, Cd3 refines as ca. 25% occupied. Similar results are also documented for $Sr_9Cd_{4.26(2)}Bi_9$ and $Ca_9Zn_{4.10(1)}Bi_9$ (Supporting Information). For some of the other studied compounds, $Yb_9Cd_{4.01(1)}Bi_9$ and $Ca_9Cd_{4.06(1)}Bi_9$ for instance, the "off-stoichiometry" is virtually absent and these trends can be accounted for based on simple geometric principles (below).

If the interstitial site were fully occupied, the ribbons in the archetype "9−4−9" would become further interconnected through the extra atom. This will give a channel-like framework with Sr^{2+} cations occupying the empty space. A similar polyanionic network exists in the structure of $Ca_3Al_2Ge_3$,[27] having the same number of atoms in the asymmetric unit as this hypothetical "9−6−9" structure, but with different connectivity of the $AlGe_4$ tetrahedra.

Structure Relationship between $Sr_9Cd_{4.49(1)}Sb_9$ and Ca_2CdSb_2. Another interesting feature of the $Sr_9Cd_{4.49(1)}Sb_9$ structure is in the way it can be related to the structure of the recently reported compound Ca_2CdSb_2.[12] The structure of the latter features silicate-like chains of $CdSb_4$ tetrahedra that are connected in a lateral direction to form infinite layers.[12] Figure 3 shows a schematic comparison between fragments of the two structures: a sequence of four corner-shared $CdSb_4$ tetrahedra from the $[Cd_4Sb_9]$ ribbons in $Sr_9Cd_{4.49(1)}Sb_9$, along with the coordination polyhedron of one of the Sr cations, is depicted in Figure 3a; Figure 3b illustrates a similar sequence cut out from the $^2_\infty[CdSb_2]$ layers in Ca_2CdSb_2, together with the polyhedron of the analogously coordinated Ca cation. Relevant distances are compared side-by-side in Table 3. The similarities and the differences become evident almost immediately—an imaginary removal of the inversion symmetry of the $[Cd_4Sb_9]$ ribbons about Sb1 and allowing the Cd1−Sb1−Cd1 angle to relax will result in a similar building block to that of Ca_2CdSb_2, depicted in Figure 3b. Incidentally, the Sb1 position in $Sr_9Cd_{4.49(1)}Sb_9$ is the one with the longest Cd−Sb distances so that the "bending" of these weaker bonds is not unjustified. To arrive at the very same topology, one needs to further "flip" the last $CdSb_4$ tetrahedron in the row (from left to right).

The cations in both structures reside in very similar polyhedra formed by the adjacent $CdSb_4$ tetrahedra. Take, for example, the strikingly similar coordination polyhedra of Sr2 and Ca2, Figure 3, parts a and b, respectively. As already discussed in an earlier publication, the Ca^{2+} cations in Ca_2CdSb_2 reside well outside the equatorial plane of the Sb octahedron, making it look more like a square pyramid. A similar distortion also exists for Sr2 in $Sr_9Cd_{4.49(1)}Sb_9$; however, the deviation from the center position in this case is not as large as it is in Ca_2CdSb_2.[12] As shown in Table 3, the corresponding distances from the two apical antimony's to Sr2 are 3.3232(11) and 3.9551(11) Å, whereas in Ca_2CdSb_2, these are 3.1323(14) and 4.102(2) Å, respectively. These differences can be attributed to the different sizes of the cations (size effects). One might then speculate that since the two formulas, $Sr_9Cd_{4.49(1)}Sb_9$ and Ca_2CdSb_2, are virtually identical (and hence the two compounds are isoelectronic), the way space can be efficiently filled with spheres of different radii will determine the preference of one structure versus another. Indeed, all attempts to synthesize $Ca_9Cd_{4.5}Sb_9$ with the $Sr_9Cd_{4.49(1)}Sb_9$ structure, or vice versa, Sr_2CdSb_2 with the Ca_2CdSb_2 structure, have proven unsuccessful. These results compliment ours and other groups' studies on the role of the cations (not only as spacers or electron donors) for the formation of intermetallic compounds with complex structures.[10,12,13,28−30] In this context, it is instructive to mention Yb_2CdSb_2, the Yb counterpart of the above-discussed Ca_2CdSb_2.[12] These two compounds crystallize in subtly different structures and present a different example of the role of the cations as structure-directing factors—after all, the ionic radii of the Yb^{2+} and the Ca^{2+} cations are nearly identical, and both compounds are expected to be isoelectronic and isostructural.

Electronic Structure and Homogeneity Range. These considerations prompt the attention to another interesting observation regarding the formal electron count and its correlation with the phase width of the series of compounds under consideration. In most simplified terms, the electron count in these systems (treating the transition metal as a closed-shell ion, i.e., Zn^{2+} or Cd^{2+} in d^{10} configuration) can be approached from the standpoint of the Zintl formalism.[9] According to this idea and excluding the partially occupied cadmium from consideration, the electron count pertinent to the anionic sublattice of the "9−4−9" structure can be described as $4 \times (Cd^{2+}) + 9 \times (Sb^{3-}) = [Cd_4Sb_9]^{19-}$. This reveals a charge imbalance because there are only 9 divalent alkaline-earth cations, i.e., there are only $9 \times 2 = 18$ positive charges. This "problem" has been previously noted and explained by the inadequacy of the Zintl concept to explain the electronic requirement of the polyanionic

(27) Cordier, G.; Schäfer, H. *Z. Anorg. Allg. Chem.* **2004**, *490*, 136−140. Note here that although $Ca_3Al_2Ge_3$ (= $Ca_9Al_6Ge_9$) is an electron precise phase, the hypothetical $Sr_9Cd_6Sb_9$ with fully occupied interstitial position would be too electron-rich.

(28) (a) Ponou, S.; Fässler, T. F.; Tobías, G.; Canadell, E.; Cho, A.; Sevov, S. C. *Chem. Eur. J.* **2004**, *10*, 3615−3621. (b) Alemany, P.; Llunell, M.; Canadell, E. *Inorg. Chem.* **2006**, *45*, 7235−7241.

(29) (a) Wu, L. M.; Kim, S.-J.; Seo, D. K. *J. Am. Chem. Soc.* **2005**, *127*, 15682−15683. (b) Tobash, P. H.; Bobev, S. *J. Am. Chem. Soc.* **2006**, *128*, 3252−3253.

(30) Bobev, S.; Bauer, E. D.; Thompson, J. D.; Sarrao, J. L.; Miller, G. J.; Eck, B.; Dronskowski, R. *J. Solid State Chem.* **2004**, *177*, 3545−3552.

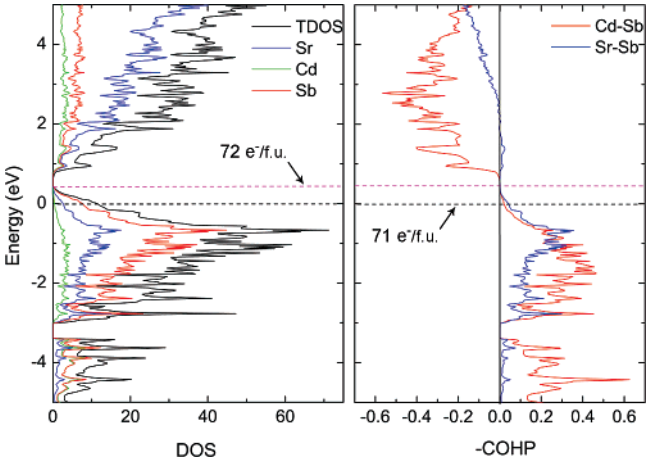

Figure 4. Projected partial DOS and COHP diagrams for selected cation−anion and anion−anion interactions in $Sr_9Cd_{4.49(1)}Sb_9$. Contributions from different atoms are color-coded. Calculations are performed on the empty "9−4−9" structure. The Fermi levels (ϵ_F) corresponding to 71 or 72 electrons per formula are depicted with a black dashed line and a pink dashed line, respectively. See text for details.

network.[13] In particular, it has been suggested that "nonclassical" structural elements such as the linear arrangement around Sb1 (above) may require less electrons so that the entire family of "9−4−9" phases will not be electron deficient.[13] The validity of such idea has recently been challenged on the example of $Yb_9Zn_4Bi_9$,[31] the Yb analog of the long-known $Ca_9Zn_4Bi_9$.[13a] Its structure has been rationalized as $(Yb^{3+})(Yb^{2+})_8([Zn_4Bi_9]^{19-})$, i.e., as a mixed-valent system with polyanionic network that requires 19 additional electrons.[31]

Not long ago, the report on nonstoichiometry in $Yb_9Zn_{4+x}Sb_9$ and $Ca_9Zn_{4+x}Sb_9$ ($x < 0.5$) has raised again the concerns about the nature of the bonding across the series.[11] This study suggests that all "9−4−9" compounds invariably contain an interstitial atom that provides up to one extra electron according to the formulation $[Cd_{4.5}Sb_9]^{18-}$. The Cd−Sb, Cd−Bi, and Zn−Bi compounds considered herein prove that such an explanation is not unique to the Zn−Sb system. The analysis of the band structure (below) provides a new insight on the phase width, the bonding, and the properties of the whole class of compounds.

Although based on the overly simplistic Zintl reasoning, the arguments presented above are fully supported by the results from the electronic structure calculations (Figure 4). From the plot of the projected DOS (density of states), it is evident that the Fermi level of $Sr_9Cd_4Sb_9$ (i.e., $Sr_9Cd_{4+x}Sb_9$ where $x = 0$) falls in a region of low, but not negligible, DOS. This suggests that such stoichiometric compound should exhibit metallic behavior. Assuming a rigid band model and filling one more electron (by virtue of adding interstitial atoms; cation mixed valency is ruled out here) moves the Fermi level to a small gap (Figure 4). This electron count corresponds to a composition $Sr_9Cd_{4.5}Sb_9$, i.e., x equals exactly 0.5. Such compound is expected to be a narrow-gap semiconductor. If $Sr_9Cd_{4+x}Sb_9$ has a certain phase width and can exist for various "x", ranging from 0 to 0.5, then one can speculate that such phases will also be metallic. Although there is no indication that $Sr_9Cd_{4.49(1)}Sb_9$ has a wide homogeneity range and no direct evidence from electrical resistivity measurements is available (due to our inability to measure very air sensitive samples), these assumptions are consistent with the poorly metallic properties of the isostructural $Ca_9Zn_{4+x}Sb_9$ ($x \approx 0.47$).[11]

Calculations for the rare-earth metal analogs reveal similar trends—with almost 14 electrons filling the 4f shells, the Yb f-states in $Yb_9Cd_{4+x}Bi_9$ could be basically considered as localized core states, i.e., the Yb cations, as expected, are divalent ($[Xe]f^{14}$). The major difference in this case is that the Fermi level shifts right above the f-bands, and as a result of this, the band gap nearly vanishes. The divalent Yb and Eu[32,33] were confirmed by the experimentally determined magnetic susceptibilities (Figure 5); the temperature dependence of the resistivity of $Eu_9Cd_{4.21(1)}Bi_9$, which reveals metallic behavior (room-temperature resistivity of about 1.5 mΩ·cm—see the Supporting Information), corroborates the predicted metallic properties as well.

The corresponding COHP (crystal Hamilton orbital population—Figure 4, right) indicates that for $Sr_9Cd_{4+x}Sb_9$ ($x \neq 1/2$), the Fermi level cuts through bands contributed predominantly by Sr's 4d and Sb's 5p states. This is not unprecedented, since p−d mixing of cation's and anion's states has recently been shown to be quite common for many "classic" Zintl phases.[34] The COHP curves for the average Sr−Sb and Cd−Sb interactions also clarify another important point that was previously discussed—the apparent electron deficiency in the "9−4−9" system. Indeed, the small bonding areas just above the Fermi level in the COHPs of Sr−Sb and Cd−Sb suggest that the bonding is not optimized with the available 71 electrons. On the other hand, the bonding optimizes and the system achieves lower energy with 72 electrons. This exact balance can be achieved by adding precisely 0.5 additional Zn or Cd per formula unit. However, the experiments confirm that it is possible for the structure to exist with *lesser*, or even *without* any discernible amount of additional Cd or Zn. This means that simplifying the bonding in these systems in terms of covalent polyanionic ribbons, $[Cd_{4+x}Sb_9]^{19-2x}$ ($x \leq 0.5$), and spectator cations that supply electrons is unjust. Evidently, small departures from the ideal electron concentration are possible, and most likely, they are compensated by the lattice energy. Cases like that are rare in Zintl phases, where the electronic requirements are the dominating factor; however, recent studies on various

(31) Kim, S.-J.; Salvador, J.; Bilc, D.; Mahanti, S. D.; Kanatzidis, M. G. *J. Am. Chem. Soc.* **2001**, *123*, 12704−12705.

(32) $Yb_9Cd_{4.01(1)}Bi_9$ exhibits a weak paramagnetic behavior in the temperature range of 5−290 K (Figure 5a). The susceptibility data can be fit to the modified Curie−Weiss law, which yields a small effective moment of ca. 0.35 μ_B per Yb. This is most likely due to an impurity and not to intrinsic trivalent Yb^{3+} (4.54 μ_B) (ref 33). These results are consistent with our previous work on $Yb_9Zn_{4+x}Sb_9$ ($0.2 < x < 0.5$) (ref 11), which supports such conclusion and calls into question the reported mixed valency in the third known Yb compound with this structure, $Yb_9Zn_4Bi_9$ (ref 31). A careful reexamination of the temperature dependence of the magnetic susceptibility of this phase indicates that it also exhibits a weak paramagnetic behavior (Figure 5b). Fit of the data to the modified Curie−Weiss law results again in rather small effective moment of 0.2 μ_B per Yb ion. This fails to confirm the previously reported magnetic moment and the accompanying structure rationalization (ref 31). The third lanthanide-based compound, $Eu_9Cd_{4.21(1)}Bi_9$, as expected, is paramagnetic in the temperature range of 20−290 K. The temperature dependence of the molar susceptibility follows the Curie−Weiss law, and a fit of the inverse susceptibility $1/\chi(T)$ to a line readily yields an effective moment of 7.86 μ_B per Eu (free ion Eu^{2+} has an effective moment of 7.94 μ_B) (ref 33). At around 11 K, the spins order in an antiferromagnetic fashion with a Weiss temperature of about −12 K. These results indicate that the Yb or Eu cations should both be divalent. These results are corroborated by the electronic structure calculations.

(33) Smart, J. S. *Effective Field Theories of Magnetism*; Saunders: Philadelphia, PA, 1966.

(34) (a) Li, B.; Mudring, A.-V.; Corbett, J. D. *Inorg. Chem.* **2003**, *42*, 6940−6945. (b) Mudring, A.-V.; Corbett, J. D. *Inorg. Chem.* **2005**, *44*, 5636−5640. (c) Mudring, A.-V.; Corbett, J. D. *J. Am. Chem. Soc.* **2004**, *126*, 5277−5281. (d) Li, B.; Corbett, J. D. *Inorg. Chem.* **2005**, *44*, 6515−6517.

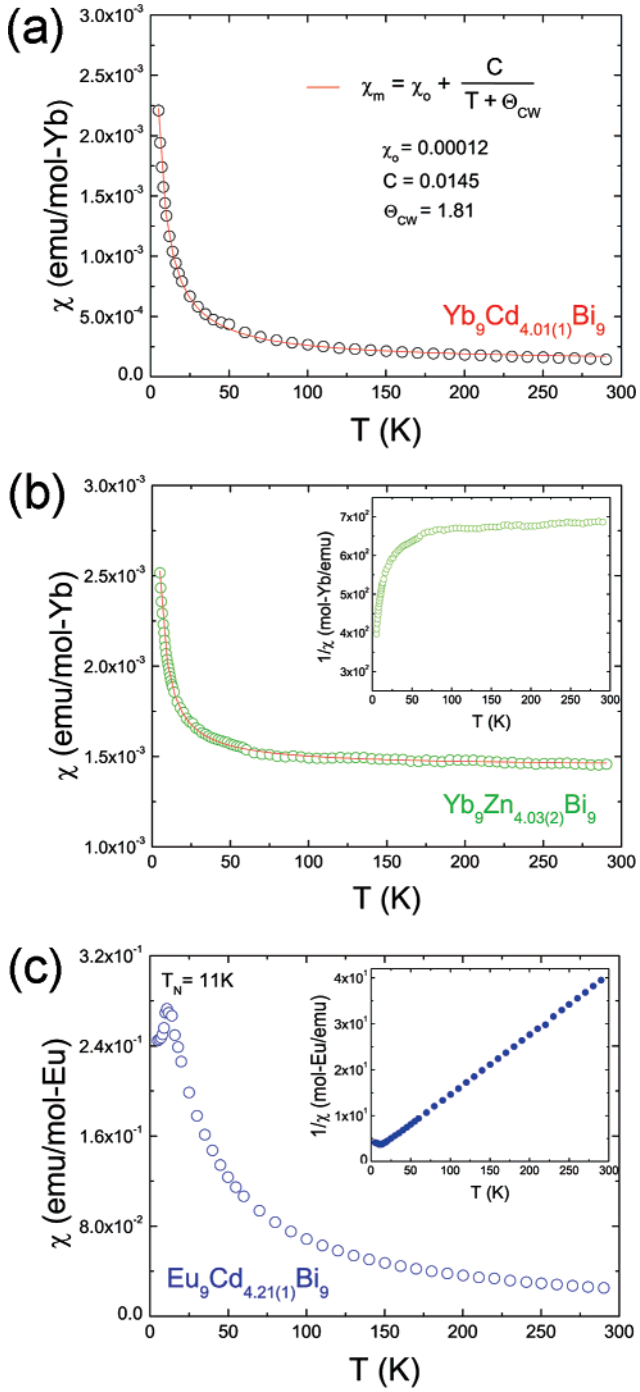

Figure 5. Temperature dependence of the magnetic susceptibility (χ_m) of $Yb_9Cd_{4.01(1)}Bi_9$ (a), $Yb_9Zn_{4.03(2)}Bi_9$ (b), and $Eu_9Cd_{4.21(1)}Bi_9$ (c) measured in an applied field of 500 Oe. Inset in (b) shows $1/\chi_m$ as a function of the temperature and the inability to fit the data for the Yb compounds to the Curie−Weiss law; inset in (c) shows the linear fit of $1/\chi_m$ to the Curie−Weiss law.

three-dimensional networks suggest that the packing (size effects) may take priority over the electronic effects in governing the formation of complex intermetallics.[10,12,32]

Generalized Structure Map. From all of the above, the structure, the electronic structure, and the physical properties of the title compounds can be explained and understood. However, the question why the occupancies of the interstitial transition metal vary so sporadically and seemingly with little dependence on the reaction conditions has not been answered

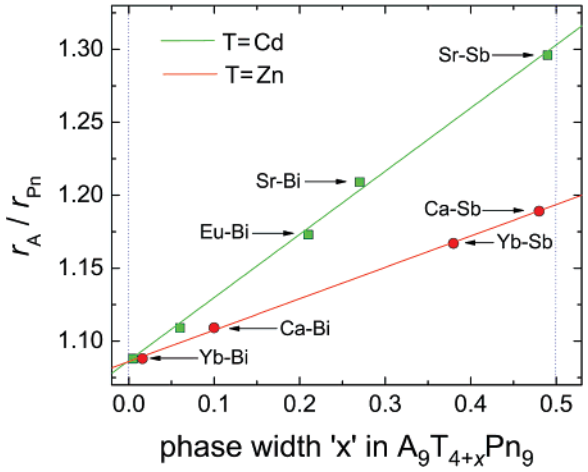

Figure 6. Structure map for $A_9Zn_{4+x}Pn_9$ and $A_9Cd_{4+x}Pn_9$ ($0 < x < 0.5$; A = Ca, Sr, Eu, Yb; Pn = Sb, Bi) phases. Plotted are the dependences of the refined occupancies of the interstitial Cd3 or Zn3 atoms vs the ratio r_A/r_{Pn} for both the Cd and Zn compounds. The Pauling's metallic radii (r) are used for this comparison. Standard deviations are smaller than the symbols used.

yet—after all, the electron provided by the extra Cd or Zn seems to be necessary in order for the system to achieve the optimal electron concentration. To answer this question and to find out what governs this phenomenon, we analyzed the size of the constituent elements and plotted the occupancy of the interstitial atom as its function (Figure 6). The rationale behind this plot is the following—as already mentioned, the partially occupied Cd or Zn site is located inside a tetrahedron formed by the pnicogens, which in turn is superimposed on a trigonal prism of the alkaline- or rare-earth cations. This "empty" space is rather tight and may not be suitable to accommodate an additional atom that is too large to fit in. An easy way to increase the effective volume of this "cavity" will be using bigger cations since they will require bigger separation and will make more room for larger interstitial atoms or can lead to a higher occupancy. However, cations that are too big, such as Ba^{2+}, may prove impossible to pack in an array of corner-shared tetrahedra of Sb or Bi. A proof of this line of thinking is the fact that all attempts to make the Ba analogs of any of the known Ca or Sr compounds with this structure failed. Our systematic and comprehensive syntheses (using both flux and on-stoichiometry reactions) led to the discovery of several other Ba−Cd−Bi and Ba−Cd−Sb phases such as $Ba_2Cd_3Bi_4$,[8b] $Ba_{11}Cd_8Bi_{14}$,[8c] $Ba_{21}Cd_4Sb_{18}$,[35] and $Ba_{11}Cd_6Sb_{12}$.[35] Analogously, smaller cations will have an inverse effect on the size of the interstitial opening (note that the "9−4−9" structure with As is not reported as of the time of writing of this article). Evidently, there will be an optimal balance between the sizes of the constituent atoms and the ratio of the cation to pnicogen radii will play a direct role in determining the ability of this "cavity" to accept atoms.

Figure 6 presents a straightforward view of the above-described relationships. The Pauling's metallic radii (r),[36] or rather the ratios of r_A/r_{Pn} for both the Cd and Zn compounds, are plotted as a function of the maximum occupancy of the interstitial site (predicted by theory not to exceed 25% of the 4*g* site). As shown in the figure, the dependence is smooth and

(35) Xia, S.-Q.; Bobev, S. Unpublished results.
(36) Pauling, L. *The Nature of the Chemical Bond*; Cornell University Press: Ithaca, NY, 1960.

nearly linear. Several "real" crystal structures are compared and contrasted using the plot, confirming the strong "size preference" for each combination. One also immediately notices that, on average, the Zn compounds tend to have higher occupancies than the Cd compounds, which is easy to understand since Zn is smaller than Cd and therefore should be easier to fit in the empty space.

The biggest advantage of such a "structure map" is that it can also be used as a guide in the planned synthesis (design) of new compounds. To illustrate that simply, we can point out the hypothetical $Ca_9Cd_{4+x}Sb_9$ and $Yb_9Cd_{4+x}Sb_9$ compounds. The structure map predicts them to be stable for $x \approx 0.2$; however, their experimentally determined structures, Ca_2CdSb_2 and Yb_2CdSb_2, respectively,[12] are slightly different than the "9−4−9" type described herein. The parallel between $Ca_9Cd_{4+x}Sb_9$, exemplified by $Sr_9Cd_{4.49(1)}Sb_9$ and Ca_2CdSb_2, was already discussed; we note again that realizing the delicate size requirements and the fact that $Ca_9Cd_{4.22}Sb_9$ will have slightly "unoptimized" bonding (Figure 6), one might speculate that it will have higher energy compared to Ca_2CdSb_2. Such energy difference is the driving force for the preferred formation of Ca_2CdSb_2 versus the predicted $Ca_9Cd_{4.22}Sb_9$. Similar arguments can also be made for the Yb_2CdSb_2−$Yb_9Cd_{4.18}Sb_9$ counterparts. Since the arrangements of the polyanionic layers in both Ca_2CdSb_2 and Yb_2CdSb_2 are very sensitive to the cations' size, even for Sr, these structures have to break and make the anionic units more flexible in adopting bigger cations.

Conclusions

Seven compounds, $Sr_9Cd_{4+x}Sb_9$, $A_9Zn_{4+x}Bi_9$, and $A_9Cd_{4+x}Bi_9$ ($0 < x < 0.5$; A = Ca, Sr, Eu, Yb) have been synthesized and structurally characterized. Their structures feature unique one-dimensional $[Cd_4Sb_9]$, $[Zn_4Bi_9]$, and $[Cd_4Bi_9]$ ribbons, respectively, that are made of transition metal centered tetrahedra of the pnicogens, connected via corner sharing. The ribbons run parallel to the direction of the shortest crystallographic axis, and at least formally, such atomic arrangement can be assigned to the $Ca_9Mn_4Bi_9$ type. Nonetheless, there is an additional, albeit partially occupied site, which has been overlooked in some earlier publications and which explains the narrow homogeneity range.

Our study suggests that that all members of this family invariably contain such an interstitial atom that provides up to one extra electron for the bonding. The analysis of the electronic structure confirms that the structure is flexible in a sense it can adapt to small deviations from the ideal electron concentration, which is apparently compensated by the lattice energy. Such examples, where the size effects take priority over the electronic requirements in governing the stability of Zintl phases, are rare and compliment previous studies on the role of the cations (not just as "spectators" or "electron donors") for the formation of intermetallic compounds with complex structures.

Acknowledgment. Dedicated to the memory of the victims of the tragic events at Virginia Tech. Svilen Bobev acknowledges financial support from the University of Delaware through a start-up Grant. We are indebted to Arif Ozbay and Professor Edmund R. Nowak from the Department of Physics and Astronomy for their help with the four-probe resistivity measurements.

Supporting Information Available: Details on the synthesis and the crystallographic studies for all Bi compounds, tables with crystallographic data for all, including $Sr_9Cd_{4.49(1)}Sb_9$ synthesized from lead flux, all X-ray crystallographic files in CIF format, along with graphical representations of the crystal structures with anisotropic displacement parameters, Fourier maps and disorder modeling. This material is available free of charge via the Internet at http://pubs.acs.org.

JA0728425